Amphiphilic Asymmetric Comb Copolymer with Pendant Pyrene Groups and PNIPAM Side Chains: Synthesis, Photophysical Properties, and Self-Assembly

Chuanzhuang Zhao, Dongxia Wu, Xueming Lian, Yue Zhang, Xiaohui Song, and Hanying Zhao*

Key Laboratory of Functional Polymer Materials, Ministry of Education, Department of Chemistry, Nankai University, Tianjin 300071, P. R. China

Received: January 26, 2010; Revised Manuscript Received: March 29, 2010

An amphiphilic asymmetric comb polymer with pendant pyrene groups and poly(*N*-isopropylacrylamide) (PNIPAM) side chains was synthesized based on click chemistry and reversible addition−fragmentation chain transfer polymerization. Gel permeation chromatography, FTIR, and ^{1}H NMR results all indicated successful synthesis of a well-defined comb polymer. The photophysical properties and self-assembly of the polymer in solution were studied by UV−vis spectroscopy, fluorescence technique, and transmission electron microscopy. The intensity ratio of the excimer peak (I_E) to the monomer peak (I_M) of the comb polymer in THF was used to monitor the formation of inter- or intramolecular excimers. At low polymer concentration, the value of I_E/I_M kept unchanged, indicating the formation of intramolecular excimer; at high polymer concentration, the value increased rapidly with concentration because of the formation of intermolecular excimer. The change of the intensity ratio of the first to the third vibronic band (I_1/I_3) on the monomer emission of the comb polymer also proved the association of the pendant pyrene groups in THF at high polymer concentration. In aqueous solution, the comb polymer chains self-assembled into vesicles with pyrene groups in the walls and PNIPAM side chains in the coronae. The value of the critical aggregation concentration of the polymer was determined by fluorescence technique. Temperature exerted a significant effect on the size and morphology of the vesicles. At a temperature above the lower critical solution temperature (LCST) of PNIPAM, PNIPAM brushes in the coronae of vesicles collapsed on the surface of the structures forming nanosized domains, and vesicles with smaller size were obtained. Fluorescence quenching experiments indicated that the collapsed PNIPAM chains protected a part of pyrene groups from being quenched by nitromethane at a temperature above the LCST of PNIPAM.

1. Introduction

The thermal-responsive behavior of poly(*N*-isopropylacrylamide) (PNIPAM) in aqueous media has attracted increasing interest since it was first reported by Heskins and Guillet.[1] The polymer undergoes the conformational transition from hydrated coil to dehydrated globule in water at around 32 °C, which is also known as lower critical solution temperature (LCST) behavior.[1−4] Due to its thermal-responsive property, the polymer is widely used in optical/electronic devices,[5,6] biomedical systems,[7,8] responsive surfaces,[9,10] and chemosensors.[11,12] Fluorescence technique is a powerful tool in the study of conformation change of polymer chains at a molecular level. To study the physical properties of PNIPAM using the fluorescence technique, fluorescent groups have been incorporated into PNIPAM chains.[13−15] However, most of these studies focused on linear fluorophore-decorated PNIPAM. The fluorophore-decorated PNIPAM with nonlinear topological structures have not been extensively studied.

Comb polymers, also called macromolecular brushes or bottle brushes, are one type of nonlinear polymers with long densely grafted side chains on polymer backbones.[16] Because of the crowded side chains on the backbone, the comb polymers adopt a wormlike cylindrical brush conformation, in which the side chains are stretched in the direction to the backbone.[17] It has been theoretically predicted or experimentally proved that comb polymers can self-assemble into micellar,[18] vesicullar,[19] or lamellar[20] morphologies in selective solvents. These studies also revealed great potential for comb polymers in building up functional structures that are responsive to environmental stimuli.

Controlled/living radical polymerization (CRP) techniques[21] and high-efficient coupling reactions[22] are widely utilized in the synthesis of comb polymers. Among the CRP techniques, reversible addition−fragmentation chain transfer (RAFT) polymerization is the most versatile technique due to the facile experimental setup and great potential for scale-up reactions.[23] Click chemistry is an attractive coupling reaction because of the moderate reaction conditions conducted in multiple solvents, tolerance to numerous functional groups, high yields, and little or no side reactions.[24−26] A variety of functional polymers with different structures can be prepared based on a combination of RAFT polymerization and click chemistry. In previous papers, we reported the synthesis of fluorophore-decorated comb copolymers and thermal-responsive comb polymers based on RAFT polymerization and click chemistry.[27]

The asymmetric comb polymer is a type of comb polymer with two different side chains (or functional groups) on each repeating unit of the backbone. Asymmetric macromolecular brushes have well-defined structures and many interesting properties. In this paper, we report the synthesis of comb polymers with pendant pyrene groups and PNIPAM side chains

* Corresponding author. Tel.: 86-022-2349-8703. E-mail: hyzhao@nankai.edu.cn.

10.1021/jp1007494 © 2010 American Chemical Society
Published on Web 04/26/2010

SCHEME 1: Scheme for the Synthesis of the Amphiphilic Comb Polymer with Hydrophilic Poly(*N*-isopropyl acrylamide) (PNIPAM) Side Chains and Hydrophobic Pyrene Groups Based on Click Chemistry and RAFT Polymerization

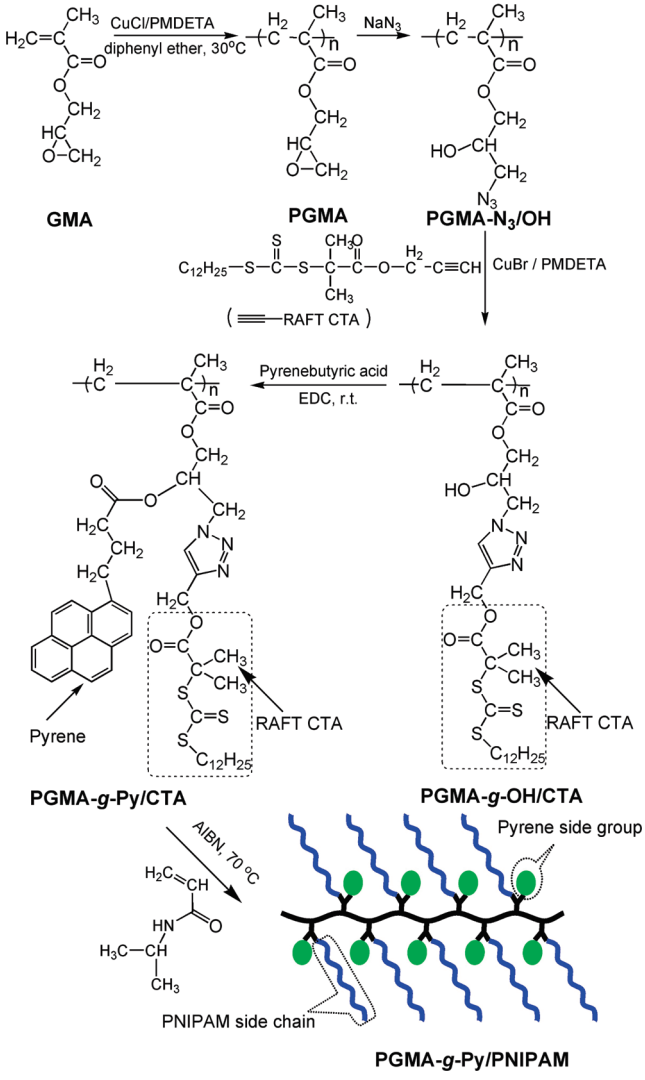

by RAFT polymerization and click chemistry. Polymer backbones with pendant hydroxyl groups and azide molecules were synthesized by atom transfer radical polymerization (ATRP) of glycidyl methacrylate (GMA) and ring-opening reaction. The RAFT chain transfer agent (CTA) and pyrene groups were grafted to the polymer backbone by a facile click reaction and esterification reaction, respectively. PNIPAM side chains were prepared by RAFT polymerization. The synthesis was outlined in Scheme 1. The amphiphilic comb polymer has hydrophilic thermal-responsive PNIPAM side chains and hydrophobic backbone and pendant fluorescent groups. The photophysical properties of the polymer in good solvent (tetrahydrofuran, THF) and in selective solvent (water) were studied by fluorescence technique. The self-assembly and LCST behavior of the polymer in aqueous solutions were studied by transmission electron microscopy (TEM), microdifferential scanning calorimetry (micro-DSC), and dynamic light scattering (DLS). The thermal responsibilities of self-assembly aggregates to outside stimuli were also studied.

2. Experimental Section

Materials. Glycidyl methacrylate (Aldrich, 97%) was purified by distilling under reduced pressure. *N*-Isopropyl acrylamide (97%) was purchased from Aldrich, and before use it was recrystallized from hexane and dried under vacuum. Copper bromide (CuBr, 99.5%) and copper chloride (CuCl, 97%) were purchased from Guo Yao Chemical Company and TianJin Institute of Chemical Agents, respectively. Before use, they were purified by washing with glacial acetic acid and ethyl ether and drying under vacuum. $CuCl_2$ was purchased from TianJin Ke Mi Ou Chemical Company, and before use it was dried under vacuum. Disodium ethylenediamine tetraacetate (EDTA, 99%), ethyl 2-bromoisobutyrate (EBrIB) (Aldrich), pyrenebutyric acid (Alfa), 1-ethyl-3-(3-dimethylaminopropyl) carbodiimide (EDC) (Alfa), 4-(dimethylamino) pyridine (DMAP) (Alfa, 99%), sodium azide (Alfa, 99%), and *N*,*N*′,*N*″,*N*″′-pentamethyldiethylenetriamine (PMDETA) (Aldrich, 99%) were used as received. All the solvents were distilled before use.

Preparation of RAFT Chain Transfer Agent. Alkyne-terminated *S*-1-dodecyl-*S*′-(α,α′-dimethyl-α″-propargyl acetate) trithiocarbonate was synthesized by esterification of *S*-1-dodecyl-*S*′-(α,α′-dimethyl-α″-acetic acid) trithiocarbonate and propargyl alcohol. The synthesis of *S*-1-dodecyl-*S*′-(α,α′-dimethyl-α″-acetic acid) trithiocarbonate was performed according to the previous literature.[28] *S*-1-Dodecyl-*S*′-(α,α′-dimethyl-α″-acetic acid) trithiocarbonate (1.03 g, 2.75 mmol), EDC.HCl (1.08 g, 5.49 mmol), and DMAP (0.035 g, 0.27 mmol) were mixed in 20 mL of dry CH_2Cl_2. Propargyl alcohol (0.30 mL, 5.17 mmol) was added dropwise to the mixture at 0 °C. After addition, the transparent yellow solution was stirred at room temperature for 48 h. The reaction mixture was washed with distilled water three times. The ester was further purified with silica column chromatography (eluent: a mixture of petroleum ether and ethyl acetate with a volume ratio of 1:1), and *S*-1-dodecyl-*S*′-(α,α′-dimethyl-α″-propargyl acetate) trithiocarbonate was obtained.

^{1}H NMR, δ (400 MHz, $CDCl_3$, TMS, ppm): 4.69 ($-CH_2-C\equiv CH$, s, 2H); 3.25 ($-S-CH_2-CH_2-$, t, 2H); 2.46 ($-C\equiv CH$, s, 1H); 1.71 ($-CO-C(CH_3)_2-COO-$, s, 6H); 1.25−1.66 ($-C_{10}H_{20}$, m, 20H); 0.88 ($-CH_2-CH_3$, t, 3H). IR (KBr) (Wavenumber, cm^{-1}): 3302 (≡C−H), 2919 and 2850 (C−H), 2132 (C≡C), 1736 (C═O), 1069 (C═S). ESI-MS (*m*/*z*): 391.47 ($M + H^+$), 390.35 (M^+).

ATRP of GMA. PGMA was prepared by ATRP. The procedure was described as follows. Degassed GMA monomer (2.0 mL, 14.60 mmol), PMDETA (0.084 mL, 0.41 mmol), CuCl (0.036 g, 0.36 mmol), $CuCl_2$ (0.0055 g, 0.04 mmol), and diphenyl ether (4.0 mL) were added to a dry Schlenk flask. After three freeze−pump−thaw cycles, ATRP initiator EBrIB (0.060 mL, 0.41 mmol) was introduced into the flask by using a degassed syringe to initiate the polymerization. The polymerization was conducted in an oil bath at 30.0 °C for 70 min. The polymerization was stopped by transfer of the flask into liquid nitrogen. The polymer solution was diluted with chloroform and extracted with aqueous solution of EDTA to remove the copper ions. The organic layer was concentrated by rotary evaporation, and the polymer was precipitated in hexane. After filtration, the polymer was dried under vacuum until a constant weight was reached. M_n = 4.4K, M_w/M_n = 1.20. ^{1}H NMR, δ (400 MHz, $CDCl_3$, TMS, ppm): 4.30, 3.83 ppm ($-CO_2CH_2-$), 3.23 ppm ($-CH-CH_2-O-$), 2.84, 2.64 ppm ($-CH-CH_2-O-$). IR (KBr) (Wavenumber, cm^{-1}): 1730 (C═O), 907 (epoxy group).

Ring Opening of PGMA by Sodium Azide. PGMA (1.01 g, 7.10 mmol of epoxide groups) was dissolved in 30 mL of dry DMF. Sodium azide (1.40 g, 21.50 mmol) and ammonium

chloride (1.15 g, 21.50 mmol) were added to the solution, and the mixture was stirred at 50 °C for 20 h. After removal of most of DMF, poly(2-hydroxy-3-azidopropyl methacrylate) was precipitated in water, filtrated, washed with water, and dried under vacuum. In the ^{1}H NMR spectrum of the polymer, the signals representing protons of epoxide disappeared completely indicating the successful azidation procedure. On a polymer chain there are hydroxyl groups and pendant azide molecules, and the polymer was denominated as PGMA−OH/N_3. ^{1}H NMR δ (400 MHz, DMSO, TMS, ppm): 3.73−4.07 ppm (−COOC***H***$_2$−, −COOCH$_2$C***H***−OH). IR (KBr) (Wavenumber, cm^{-1}): 3472 (OH), 2104 (C−N═N═N), 1730 (C═O).

Grafting of RAFT CTA onto PGMA−OH/N_3 by Click Reaction. PGMA−OH/N_3 (0.31 g, 1.62 mmol of azide groups), alkyne-terminated RAFT CTA *S*-1-dodecyl-*S*′-(α,α′-dimethyl-α″- propargyl acetate) trithiocarbonate (1.30 g, 3.24 mmol of alkyne groups), and PMDETA (0.35 mL, 1.62 mmol) were mixed in 6.5 mL of dry DMF. The mixture was degassed by three freeze−pump−thaw cycles. CuBr (0.24 g, 1.62 mmol) was added to the solution in nitrogen atmosphere, and the mixture was stirred at room temperature for 24 h. After reaction, the solution was concentrated by rotary evaporation, and the polymer bearing CTA (PGMA−OH/CTA) was precipitated in hexane. PGMA−OH/CTA was extracted with hexane to remove unreacted RAFT CTA. M_n = 8.4K, M_w/M_n = 1.42. ^{1}H NMR δ (400 MHz, $CDCl_3$, TMS, ppm): 7.89 (triazole, 1H); 5.19 (−OCO−C***H***$_2$−triazole−, 2H), 4.83−3.72 (−OCO−C***H***$_2$−C***H***(O***H***)−C***H***$_2$−triazole, 6H), 3.24 (−SCS−S−C***H***$_2$−, 2H). IR (KBr) (Wavenumber, cm^{-1}): 1732 (C═O), 1062 (C═S).

Grafting of Pyrene Groups onto the PGMA−OH/CTA Backbone. The hydroxyl groups on PGMA−OH/CTA were used to react with pyrenebutyric acid in the presence of EDC and DMAP in CH_2Cl_2. PGMA−OH/CTA (0.1 g), pyrenebutyric acid (0.11 g, 0.37 mmol), and DMAP (2.4 mg, 0.018 mmol) were dissolved in dry CH_2Cl_2 (15 mL), and the mixture was cooled to 0 °C under stirring. EDC (0.074 g, 0.37 mmol) was added to the solution. After stirring at 0 °C for about 20 min, the solution was warmed to room temperature and stirred for 48 h. After evaporation of the solvent, the crude product was precipitated in hexane to obtain the polymer with pendant pyrene groups and RAFT CTA on the backbone (PGMA-*g*-pyrene/CTA).

Synthesis of Amphiphilic Asymmetric Comb Polymer. PGMA-*g*-pyrene/CTA was used as macro-CTA in the synthesis of PNIPAM side chains. PGMA-*g*-pyrene/CTA (12.5 mg) and NIPAM (0.17 g, 1.53 mmol) were dissolved in dry DMF (1.2 mL). AIBN (0.5 mg) was dissolved in dry DMF (2.0 mL), and then 0.84 mL of the AIBN solution was added into the monomer solution. The mixture was degassed by three freeze−pump−thaw cycles and stirred at 70 °C for 8 h. After the reaction, the polymer solution was concentrated and precipitated in hexane. The chemical structure and the side chain length of PNIPAM were determined by ^{1}H NMR. The comb polymer with a PNIPAM side chain and pendant pyrene group on every repeating unit was assigned as PGMA-*g*-pyrene/PNIPAM$_m$, where m is the average polymerization degree (DP$_n$) of PNIPAM side chains.

Characterization. ^{1}H NMR spectra of RAFT CTA and polymers were recorded on a Varian UNITY-plus 400 spectrometer using d_6-DMSO or $CDCl_3$ as the solvents. The apparent molecular weight (M_n) and molecular weight distribution (M_w/M_n) of the polymer were determined with a gel permeation chromatograph (GPC) equipped with a Waters 717 autosampler, Waters 1525 HPLC pump, three Waters UltraStyragel columns with 5K−600K, 500−30K, and 100−10K molecular ranges, a Waters 2414 refractive index detector, and a Waters 2487 dual λ absorbance detector. THF was used as eluent at a flow rate of 1.0 mL/min. Molecular weights were calibrated on PS standards. Fourier transform infrared absorption spectra (FTIR) were obtained on a Bio-Rad FTS 6000 system using diffuse reflectance sampling accessories. Mass spectra (MS) were recorded using a Thermofinnigan LCQ Advantage mass spectrometer. Ultraviolet−visible (UV−vis) absorption spectra were recorded on a Shimadzu UV-2450 spectrophotometer using a quartz cell of 1 cm path length. The scanning speed was set at 200 nm/min. TEM images were obtained on a Tecnai G2 20 S-TWIN electron microscope equipped with a model 794 CCD camera (512 × 512) at an operating voltage of 200 kV. The TEM specimens were prepared by depositing aqueous solutions of polymers on Formvar coated grids, and water was evaporated in air. The TEM specimens were stained by RuO_4. The hydrodynamic diameters (D_h) of self-assembly aggregates were measured using a Zetasizer Nano ZS from Malvern Instruments equipped with a 10 mW HeNe laser at a wavelength of 633 nm. Measurements were performed at different temperatures and analyzed in CONTIN mode. The micro-DSC measurements were performed on a VP-DSC microcalorimeter (MicroCal Inc.). Steady state fluorescence spectra were recorded on a Shimadzu RF-5301PC fluorescence spectrophotometer. The excitation and emission slits were both set at 5 nm. The excitation wavelength of the emission spectra was set at 343 nm. Samples for fluorescence measurements were prepared from stock solutions in THF (1 g/L). Aliquots of the stock solutions were diluted by THF or water to the desired concentration. Aqueous solutions were obtained by dialysis of the polymer solutions against doubly distilled water to remove THF. Concentration of the polymer solution is also expressed in the molar concentration of pyrene moieties based on the ^{1}H NMR result.

3. Results and Discussion

Synthesis of PGMA-g-Py/PNIPAM$_{53}$. ATRP of GMA was carried out in diphenyl ether at 30 °C with CuCl/PMDETA as catalyst and EBrIB as initiator.[29] The monomer conversion reached 75% within 70 min. The ring-opening reaction of PGMA was carried out by a method similar to the previous literature.[30] ^{1}H NMR spectra of the starting polymer PGMA and its azidation product PGMA−OH/N_3 are shown in Figure 1. The signals of PGMA at 3.23, 2.84, and 2.64 ppm disappeared completely after 20 h reaction with sodium azide and ammonium chloride, which indicates the successful ring-opening reaction by the azide anion. After the reaction, new peaks of PGMA−OH/N_3 at 3.73−4.07 ppm (a, b) representing the methene protons next to the ester groups and the methine protons next to the hydroxyl groups (CO_2C***H***$_2$ and C***H***−OH), at 3.30 and 3.32 ppm (c) representing methene protons connected to azide groups (C***H***$_2N_3$), were observed. On spectrum b in Figure 1, the ratio of the peak area at δ = 3.73−4.07 ppm to that at δ = 1.6−2.1 ppm is 3:2, which proves the azidation reaction of PGMA. The success of the azidation reaction was also proved by FTIR (Figure S1 in Supporting Information). After the reaction, strong absorbance peaks representing the valence vibration of azide groups at 2104 cm^{-1}, and the vibration of hydroxyl groups at 3472 cm^{-1} were observed.

Alkyne-terminated RAFT CTA *S*-1-dodecyl-*S*′-(α,α′-dimethyl-α″-propargyl acetate) trithiocarbonate was introduced onto the polymer backbone by click reaction to obtain macro-RAFT CTA, PGMA−OH/CTA. ^{1}H NMR spectrum of alkyne-

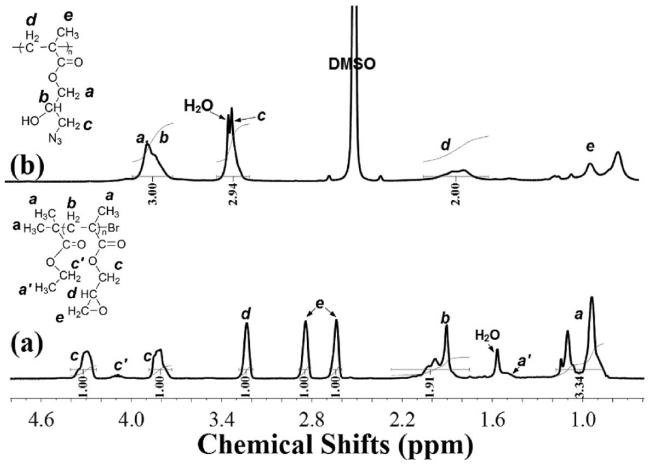

Figure 1. ^{1}H NMR spectra of (a) poly(glycidyl methacrylate) (PGMA) prepared by ATRP, and (b) its azidation product PGMA−OH/N_3 prepared by a reaction of PGMA and NaN_3 (3 equiv) and NH_4Cl (3 equiv) in DMF at 50 °C for 20 h. PGMA was measured in $CDCl_3$, and PGMA−OH/N_3 was measured in deuterated DMSO.

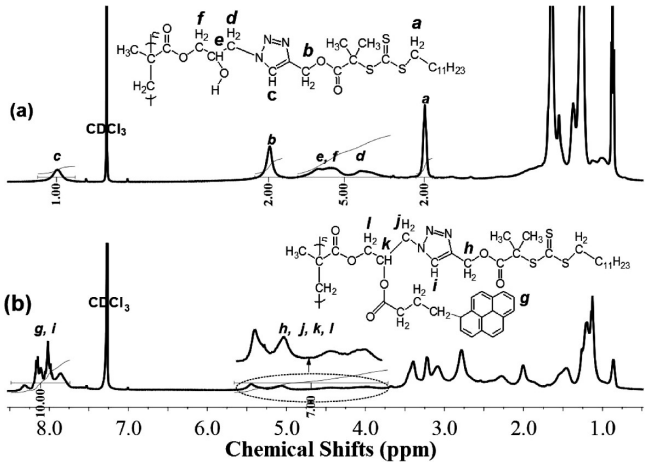

Figure 2. ^{1}H NMR spectra of (a) PGMA−OH/CTA prepared by click reaction of PGMA−OH/N_3 and *S*-1-dodecyl-*S*′-(α,α′-dimethyl-α″-propargyl acetate) trithiocarbonate and (b) PGMA-*g*-Py/CTA prepared by esterification reaction of PGMA−OH/CTA and pyrenebutyric acid.

terminated RAFT CTA was shown in Figure S2 in the Supporting Information. The RAFT CTA on the polymer backbone can be used in the synthesis of PNIPAM side chains by the "grafting from" approach. The ^{1}H NMR spectrum and peak assignments of PGMA−OH/CTA were shown in Figure 2a. After click reaction, the peak at 2.46 ppm representing the alkyne proton (−C′C***H***) disappears completely, and new peaks at 7.90 ppm (c) representing the proton on the 1,2,3-triazole ring and at 5.20 ppm (b) representing the two ester methylene protons next to the 1,2,3-triazole ring can be observed, which indicates the successful 1,3-dipolar cycloaddition reaction. The peaks at 3.72−4.83 ppm (d, e, f) correspond to the ester methylene protons, the methylene protons next to the 1,2,3-triazole ring, and the hydroxyl methine proton. The peak at 3.24 ppm (a) is attributed to the methylene protons next to the trithiocarbonate group [−C(S)S−C***H***$_2$−]. The ratio of the integral values of peak c to peak a is 1:2, indicating the success of the click reaction and the grafting of RAFT CTA to the polymer backbone (PGMA−OH/CTA).

The macro-RAFT CTA bearing pyrene groups on the polymeric backbone, PGMA-*g*-Py/CTA, was synthesized by esterification reaction of pyrenebutyric acid and PGMA−OH/

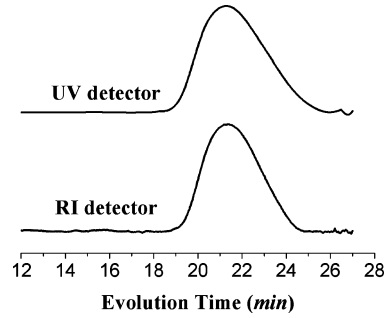

Figure 3. Gel permeation chromatograph curves of PGMA-*g*-Py/CTA recorded by an UV detector and a refractive index detector.

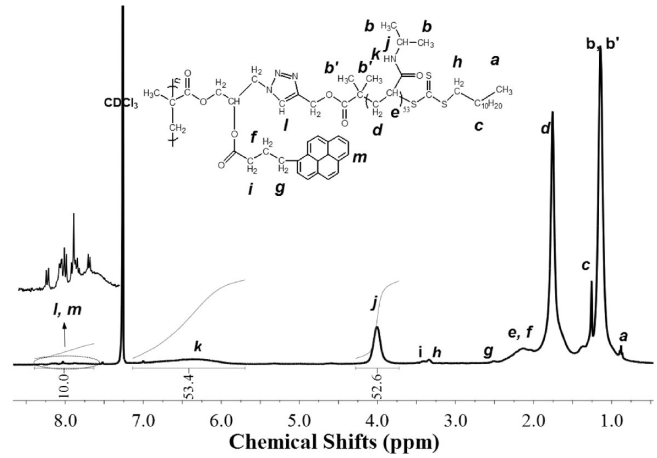

Figure 4. ^{1}H NMR spectrum of amphiphilic comb polymer with PNIPAM side chains and pendant pyrene groups, PGMA-*g*-(Py/$PNIPAM_{53}$), where 53 represents the average polymerization degree of PNIPAM side chains.

CTA. The ^{1}H NMR spectrum and peak assignments of PGMA-*g*-Py/CTA were shown in Figure 2b. After esterification reaction, new peaks at 7.3−8.5 ppm (peak g) representing the protons on pyrene groups were observed, indicating that pyrene was successfully grafted to the backbone. The peaks at 3.5−5.5 ppm (h, j, k, l) correspond to the two ester methylene protons next to the 1,2,3-triazole ring, the methylene protons next to the 1,2,3-triazole ring, the hydroxyl methine proton, and the ester methylene protons. The integral value ratio of peaks g and i to peaks h, j, k, and l is 10:7, indicating the successful esterification reaction. The success of esterification reaction was also proved by GPC measurement performed on a GPC instrument equipped with an UV detector and a refractive index detector (Figure 3). The two GPC curves agree well, which indicates that the pyrene groups were covalently bounded to the polymer chains.

PNIPAM side chains were synthesized by RAFT polymerization using PGMA-*g*-Py/CTA as macro-RAFT CTA (Scheme 1). Figure 4 shows the ^{1}H NMR spectrum of amphiphilic asymmetric comb polymer PGMA-*g*-Py/$PNIPAM_{53}$ with PNIPAM side chains and pendant pyrene groups. On the spectrum, the characteristic signals of PNIPAM at $\delta = 6.0-7.0$ ppm (peak k) representing the amide proton next to the isopropyl groups (−N***H***−CH$(CH_3)_2$) and at $\delta = 4.0$ ppm (peak j) representing methine proton on isopropyl groups (−NH−C***H***$(CH_3)_2$) were observed, which verify the successful synthesis of PNIPAM side chains. Using the ratio of the peak area at $\delta = 7.3-8.5$ ppm (l, m) to that at $\delta = 4.0$ ppm, the molar ratio of pyrene to PNIPAM and the average DP_n of PNIPAM can be calculated.

GPC traces of PGMA-*g*-Py/$PNIPAM_{53}$ and its precursors were presented in Figure 5. It can be found that the GPC trace

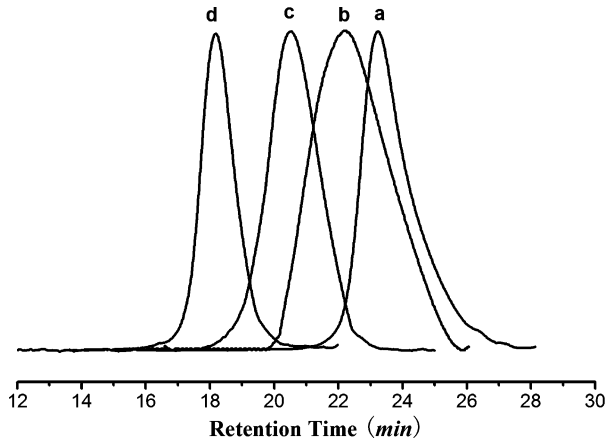

Figure 5. GPC curves of PGMA (curve a), PGMA-*g*-OH/CTA (curve b), PGMA-*g*-Py/CTA (curve c), and PGMA-*g*-Py/PNIPAM$_{53}$ (curve d).

TABLE 1: Summary of Molecular Weights and Molecular Weight Distributions of PGMA, PGMA with Pendant Hydroxyl Groups and RAFT CTA (PGMA−OH/CTA), PGMA with Pendant RAFT CTA and Pyrene Groups (PGMA-*g*-pyrene/CTA), and Amphiphilic Comb Polymer with PNIPAM Side Chains and Pendant Pyrene Groups (PGMA-*g*-Py/PNIPAM$_n$)

sample	DP$_{PNIPAM}$[a]	M_n ($\times 10^{-3}$ g mol^{-1})[b]	M_w/M_n[b]
PGMA		4.40	1.20
PGMA−OH/CTA	-	8.40	1.42
PGMA-*g*-py/CTA	-	10.7	1.27
PGMA-*g*-Py/PNIPAM$_{53}$[c]	53	26.0	1.21
PGMA-*g*-Py/PNIPAM$_{27}$	27	16.0	1.25

[a] The number-average degree of polymerization of PNIPAM side chains was measured by ^{1}H NMR. [b] Number-average molecular weight (M_n) and molecular weight distribution (M_w/M_n) were measured by gel permeation chromatography (GPC) on polystyrene standards. [c] The amphiphilic comb polymer was assigned as PGMA-*g*-Py/PNIPAM$_{53}$ in this manuscript, where 53 is the average polymerization degree of PNIPAM side chains.

moves to short retention time region after each step reaction or polymerization. The number-average molecular weights and molecular weight distributions of the products at each synthetic step and average DP$_n$ of PNIPAM side chains obtained by ^{1}H NMR are summarized in Table 1. It is noted that after ring-opening reaction the molecular weight distribution of PGMA−OH/CTA becomes broader, which is probably attributed to the hydrogen bonding formation between hydroxyl groups.

Photophysics of PGMA-g-Py/PNIPAM$_{53}$ in THF. In this research, the photophysical properties of the comb copolymers in THF, a good solvent for pyrene groups and PNIPAM side chains, were studied to obtain structural information of the polymers in solution. The influence of the concentration on the conformation of the polymer was investigated. In this paper, the concentration of the comb copolymer was converted into the molar concentration of pyrene moieties based on ^{1}H NMR results. Figure 6 shows UV−vis absorption spectra of PGMA-*g*-Py/PNIPAM$_{53}$ in THF at different concentrations. The absorption spectra present the characteristic vibronically resolved spectra of pyrene with three vibronic bands at 314, 328, and 345 nm corresponding to ^{1}La ← ^{1}A electronic transitions.[31] It can also be observed that a new peak arises at 375 nm when the concentration is above 10^{-5} M because of the association of pyrene groups at high concentration.[32]

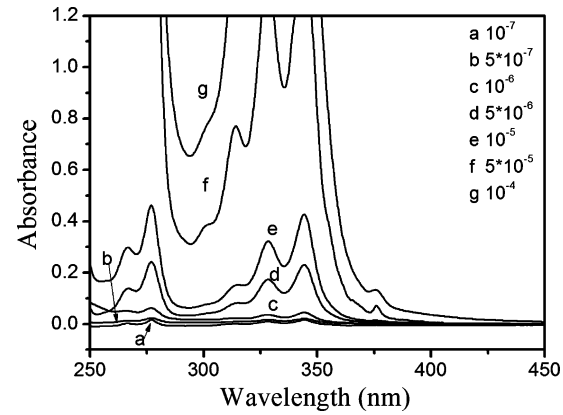

Figure 6. UV absorption spectra of PGMA-*g*-Py/PNIPAM$_{53}$ in THF at different concentrations.

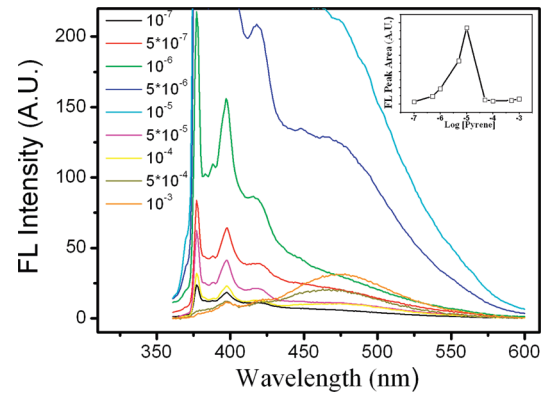

Figure 7. Fluorescence emission spectra of PGMA-*g*-Py/PNIPAM$_{53}$ in THF at different concentrations of pyrene moieties (mol/L). Excitation wavelength was set at 343 nm, and the samples were measured at 25 °C. The inset of the figure shows a plot of the peak areas of fluorescence emission vs polymer concentration.

Figure 7 shows the variable concentration fluorescence emission spectra of the comb polymer in THF at the excitation wavelength of 343 nm. The emission spectra show the typical monomer emission peaks at 377, 383, 388, 397, and 418 nm. It is noted that when the concentration is above 10^{-5} M a broad structureless band at 476 nm corresponding to pyrene excimer emission is observed. The excimer emission band originates the encounter of pyrene molecules in the excited singlet state with those in the ground state.[31] In the inset of Figure 7 the peak areas of fluorescence emission of the comb polymer are plotted against the polymer concentration. It can be seen that the peak area increases with concentration at low concentration range ($<10^{-5}$ M) and then decreases when the concentration is above 10^{-5} M. The decrease of emission intensities at high concentration is attributed to the "inner filter effect", which means that at high concentration the absorbance of the solution is so high that the emitted radiation of pyrene moieties is reabsorbed.[32,33]

It is well-known that the ratio of the intensity of the excimer peak (I_E, at 476 nm) to monomer peak (I_M, at 397 nm) can be used to measure the efficiency of inter- or intramolecular excimer formation.[31] As Figure 8 shows, the value of I_E/I_M keeps unchanged at about 0.28 when the concentration of pyrene moieties is lower than 1.7×10^{-4} M; however, when the concentration of pyrene is above this critical concentration, the value of I_E/I_M increases rapidy. For pyrene-labeled polymers, the constant value of I_E/I_M represents formation of the intramolecular excimer,[34] and in this system the encounter of two pyrene groups on the same backbone is the main reason for the excimer formation of the comb polymer in THF at low concentration.

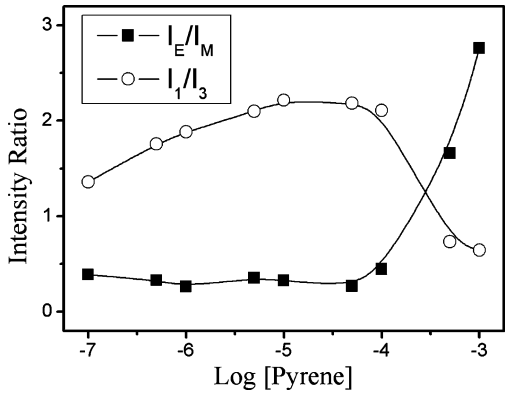

Figure 8. Plots of I_E/I_M and I_1/I_3 vs concentration of pyrene groups in PGMA-*g*-Py/PNIPAM$_{53}$.

When the concentration is above 1.7×10^{-4} M, the value of I_E/I_M increases rapidly with concentration because of the intermolecular association of pyrene moieties.[34−36]

The intensity ratio of the first to the third vibronic band (peaks at 377 and 388 nm) of monomer emission (I_1/I_3) is very sensitive to the polarity of the environment where pyrene moieties are located and can be used as a measure of solvent polarity and the interaction between pyrene molecules and the solvent.[31] The value of I_1/I_3 typically ranges from ≈1.9 in polar solvents to ≈0.6 in hydrocarbons.[37] A plot of I_1/I_3 vs pyrene concentration in THF solution is given in Figure 8. The value of I_1/I_3 initially increases with concentration. For example, it is about 1.34 at 10^{-7} M, 1.88 at 10^{-6} M, and 2.20 at 10^{-5} M. However, it decreases rapidly as the concentration is above 7.8×10^{-5} M. The slight increase of I_1/I_3 in the low concentration range implies that with the increase of polymer concentration there are more PNIPAM side chains around pendant pyrene groups and the microenvironment of pyrene moieties is more polar. The rapid decrease of I_1/I_3 beyond 7.8×10^{-5} M reflects the change of pyrene moieties from a polar environment to a nonpolar environment due to the association of pyrene groups in THF at high polymer concentration. It is worth noting that the intensity ratio reaches 0.62 at 10^{-3} M, and this value is almost the same as that of pyrene in a nonpolar hydrocarbon solvent, which further proves the association of pendant pyrene groups and the formation of a hydrocarbon microenvironment at high polymer concentration. This result coincides with the previous observation of a new peak at 375 nm in the UV absorption spectra and the rapid increase of I_E/I_M at high polymer concentration.

Self-Assembly of PGMA-g-Py/PNIPAM$_{53}$ in Aqueous Solution. Water is a good solvent for PNIPAM at a temperature below its LCST and a nonsolvent for pendant pyrene groups. So it is interesting to investigate the self-assembly of PGMA-*g*-Py/PNIPAM$_{53}$ in aqueous solution. Fluorescence emission spectra of PGMA-*g*-Py/PNIPAM$_{53}$ at different concentrations in water were obtained to determine the critical aggregation concentration (CAC) of the polymer, and the results were shown in Figure 9. It can be observed that the emission intensity increases with concentration in the low concentration range and then decreases when the concentration is beyond 10^{-5} M due to the "innner filter effect", the same phenomenon observed in THF solution. In the inset of Figure 9 the peak areas of fluorescence emission are plotted against the concentration of pyrene groups. It can be seen that the peak area increases with concentration at low concentration range and then decreases when the concentration is above 10^{-5} M. In the meanwhile, it is also noted that a strong and broad band at about 460 nm can

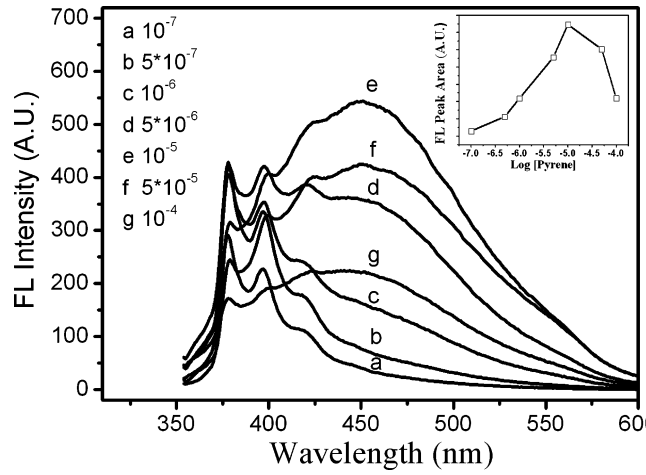

Figure 9. Variable concentration fluorescence emission spectra of PGMA-*g*-Py/PNIPAM$_{53}$ in water at an excitation wavelength of 343 nm measured at 24 °C. The inset of the figure shows a plot of the peak areas of fluorescence emission vs polymer concentration.

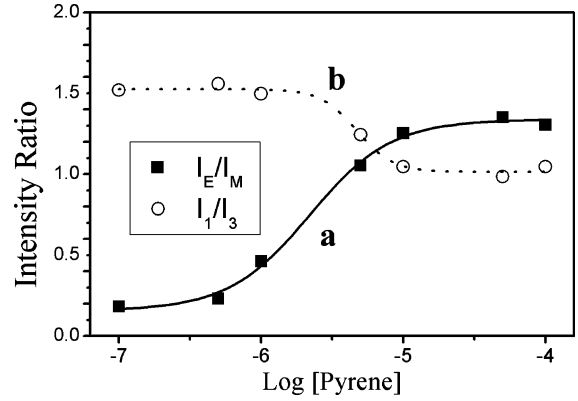

Figure 10. Excimer to monomer intensity ratio (I_E/I_M, I_E at 476 nm, and I_M at 397 nm) and the intensity ratio of the first vibronic band at 377 nm to the third one at 388 nm (I_1/I_3) of PGMA-*g*-Py/PNIPAM$_{53}$ comb polymer in aqueous solution as a function of pyrene concentration.

be observed at a concentration above 10^{-5} M, which indicates aggregation of pendant pyrene groups above CAC.

Curve a in Figure 10 is a plot of I_E/I_M as a function of the concentration of the pyrene moieties in aqueous solution. When the concentration of pyrene groups is 10^{-7} M, the value of I_E/I_M is about 0.18. I_E/I_M steadily increases with the concentration and reaches a constant value when the concentration is above 10^{-5} M. Curve b in Figure 10 shows the change of I_1/I_3 with the concentration of pyrene groups. The intensity ratio is about 1.53 in the low concentration range. When the concentration increases from 10^{-6} to 10^{-5} M, the intensity ratio decreases, and it keeps constant at 1.01 at a concentration beyond 10^{-5} M. The constant value of I_1/I_3 at high concentrations indicates the formation of multiphase structures by the comb polymer. The value of CAC set at the midpoint of the transition was calculated to be 4.6×10^{-6} M. To study the self-assembly of the comb polymer, TEM observation was conducted.

Figure 11a and b are TEM images of the self-assembled aggregates of the asymmetric comb polymer in water. The TEM specimen was prepared by depositing polymer solutions with a concentration of 10^{-5} M on Formvar coated grids at 8 °C, and water was evaporated in air. To improve the contrast, the TEM specimen was stained by RuO_4. On the TEM images, the appearance of the dark rings in the spherical structures indicates the formation of vesicular structures. The average size of the

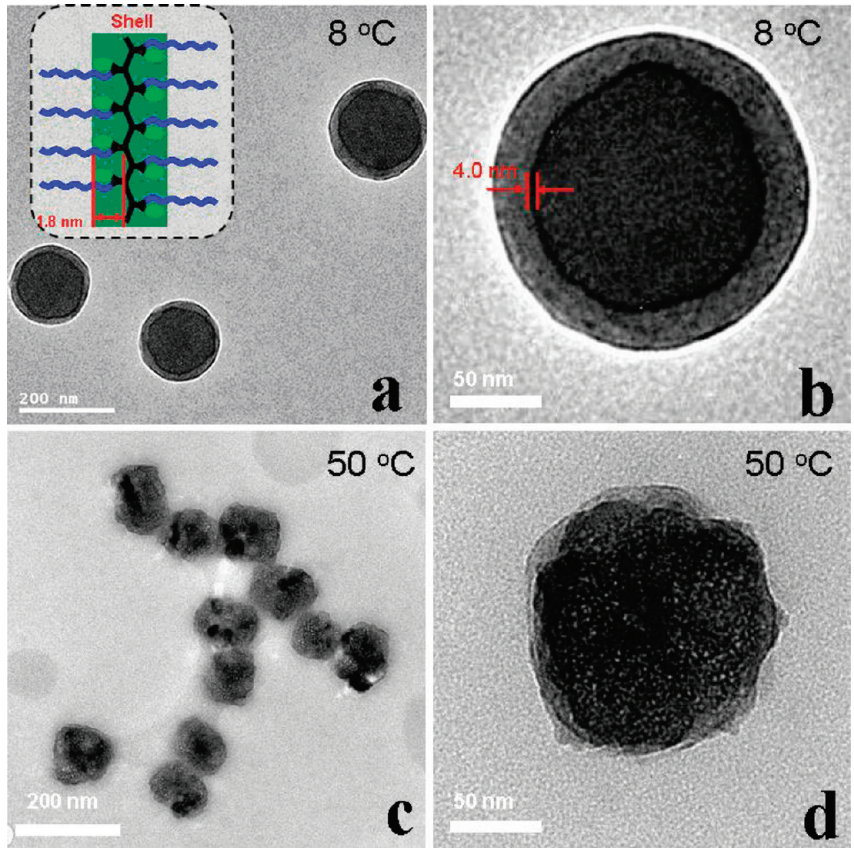

Figure 11. Transimission electron microscope images of self-assembly of PGMA-*g*-Py/PNIPAM$_{53}$ in water at 8 °C (a and b) and 50 °C (c and d). The specimens were prepared by depositing aqueous solutions on Foemvar coated copper grids at 8 and 50 °C, and the specimens were stained by RuO_4. The polymer concentration in aqueous solution is 0.1 g/L (pyrene moieties concentration is 1.5×10^{-5} M). The inset in image a shows the structure of the walls of the vesicles, and the length between a pyrene group and the backbone of the comb polymer was calculated by a Chem3D Ultra 8.0 software.

vesicular structures is about 160 nm. Although both of the PNIPAM and pyrene groups can be stained by RuO_4, pendant pyrene groups are more heavily stained due to the big aromatic rings in the structures. The dark rings composed of polymer backbone and pendant pyrene groups represent the walls of vesicles; the soluble PNIPAM side chains in the coronae of vesicles extend from the inner and outer surfaces into water to stabilize the structures. The average thickness of the wall measured on the TEM image is about 4.0 nm, and the calculated length between a pyrene group and the polymer backbone is 1.8 nm; therefore, it can be concluded that the wall of a vesicle is composed of PGMA backbones with pendant pyrene groups at two sides, as schemed in the inset of Figure 11a. The fact that pyrene groups aggregate in the hydrophobic wall agrees well with the previous fluorescence result that the value of I_E/I_M keeps at a high level after formation of the structures (curve a in Figure 10).

Thermal Response of PNIPAM Brushes on the Surfaces of Vesicles. PNIPAM is a thermosensitive polymer, which undergoes phase transition at its LCST because of the cooperative dehydration of PNIPAM chains and concomitant collapse of individual chains from hydrated coils to hydrophobic globules.[38−40] PNIPAM is soluble in cold water, but it becomes insoluble as the solution temperature exceeds its LCST. To determine the LCST of PNIPAM side chains in aqueous solution, micro-DSC measurement of the aqueous solution of PGMA-*g*-Py/PNIPAM$_{53}$ was performed. Figure 12 shows the temperature dependence of the specific heat capacity (C_p) in one heating and cooling cycle. The result shows that the sample undergoes a LCST transition at 28.0 °C in the heating process

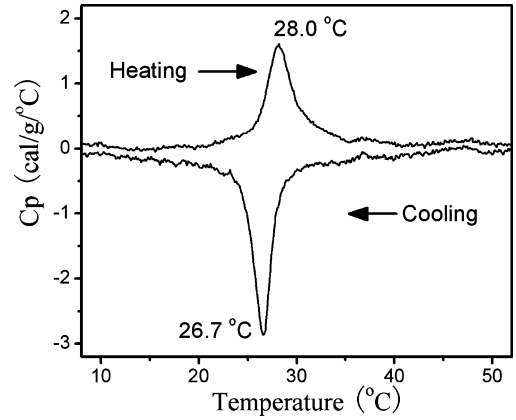

Figure 12. Microcalorimetric endotherm recorded for aqueous solution of PGMA-*g*-Py/PNIPAM$_{53}$. In the measurements, the heating rate and cooling rate were both set at 0.5 °C/min, and the polymer concentration was 5 g/L.

and at 26.7 °C in the cooling process. The difference of the two values should be attributed to some additional intrachain hydrogen bondings among PNIPAM chains formed in the collapse state at high temperatures.[41,42] The LCST of PGMA-*g*-Py/PNIPAM$_{53}$ is lower than that of the linear PNIPAM homopolymer reported in the literature,[43] which can be explained by the different structures of the polymers in aqueous solutions. In this research, PNIPAM chains are anchored to the walls of the vesicles, which is different from "free" PNIPAM homopolymer chains in aqueous solution. Zhang and co-workers prepared vesicles in water using a narrowly distributed polystyrene-*b*-

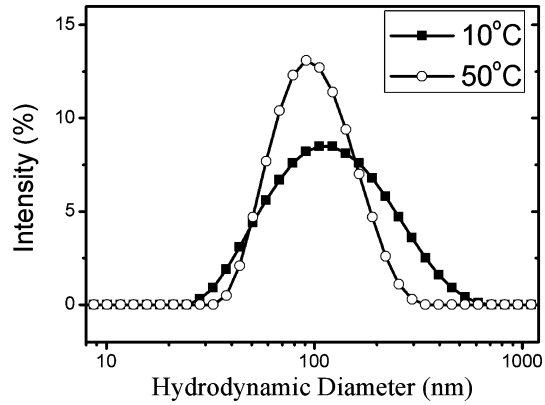

Figure 13. Size distribution of PGMA-*g*-Py/PNIPAM$_{53}$ aggregates in aqueous solution measured at 10 and 50 °C. Polymer concentration is 0.1 g/L (pyrene moieties concentration is 1.5×10^{-5} M).

poly(*N*-isopropylacrylamide) diblock copolymer, and they found that PNIPAM brushes in the coronae of the vesicles exhibit a lower shrinking temperature due to the interchain overlapping of the dense brushes on the concave surfaces of the vesicles.[44]

The morphological change of the vesicles above the LCST was also monitored by TEM. Figure 11c and d are two TEM images showing vesicles of PGMA-*g*-Py/PNIPAM$_{53}$ prepared at 50 °C. At this temperature, PNIPAM brushes collapse on the surface of the structures forming nanosized domains (Figure 11d). The contour of the structures also becomes irregular at a high temperature indicating the decrease of the stability of the structures in the aqueous solution. The TEM result also shows that the average size of the structures at 50 °C is smaller than those prepared at 8 °C due to the collapse of PNIPAM chains in the coronae of vesicular structures. The DLS result indicates that at 10 °C the average hydrodynamic diameter is about 120 nm, and it decreases to 90 nm at 50 °C (Figure 13). The decrease in the size of the vesicles is attributed to the shrinking of PNIPAM chains in the coronae.

To study the effect of temperature on the fluorescent properties of the comb polymer in aqueous solution, the fluorescence emission spectra of the polymer in aqueous solution were recorded at different temperatures (Figure S3 in Supporting Information). I_E/I_M and I_1/I_3 were also plotted against temperature. Figure 14 shows that there are no significant changes in I_E/I_M and I_1/I_3 as temperature changes from 10 to 50 °C, which means the microenvironment of pyrene moieties in the vesicles do not change with temperature and temperature does not exert an effect on the emission spectra of the comb polymer in aqueous solution. This result is different from fluorescence behaviors of many fluorophore-labeled PNIPAM homopolymers reported by other groups. In their studies, the fluorophore moieties were covalently bonded to PNIPAM chains, and the fluorescence emission spectrum has a great change at LCST of PNIPAM due to the conformation change of PNIPAM chains.[12,15] In this study, the pendant pyrene groups are "frozen" in the hydrophobic walls of vesicles, and hence the shrinking of PNIPAM brushes in the coronae does not exert influence on the microenvironment of pyrene groups.

It has been reported that in pyrene-labeled PNIPAM aqueous solution, PNIPAM chains can protect pyrene moieties from being quenched by water-soluble quenchers. The quenching effect can be illustrated by the modified Stern−Volmer model[14]

$$\frac{I_0}{I} = \left[1 - \frac{f_a K_{SV}[Q]}{1 + K_{SV}[Q]}\right]^{-1} \quad (1)$$

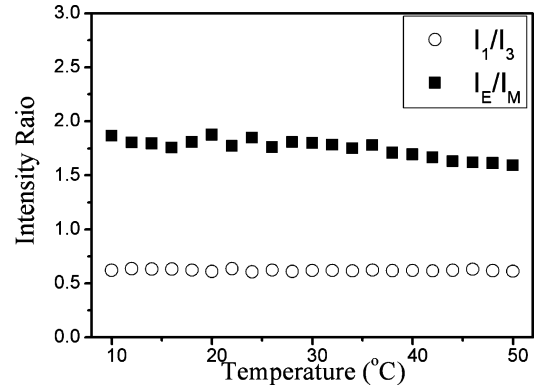

Figure 14. Excimer to monomer intensity ratio (I_E/I_M, I_E at 476 nm and I_M at 397 nm) and the intensity ratio of the first vibronic band at 377 nm to the third one at 388 nm (I_1/I_3) for 343 nm excitation spectra in aqueous solution of the comb polymer as a function of temperature. In the measurements, the heating rate was set at 0.5 °C/min, and the polymer concentration was 0.068 g/L (pyrene moiety concentration is 10^{-5} M).

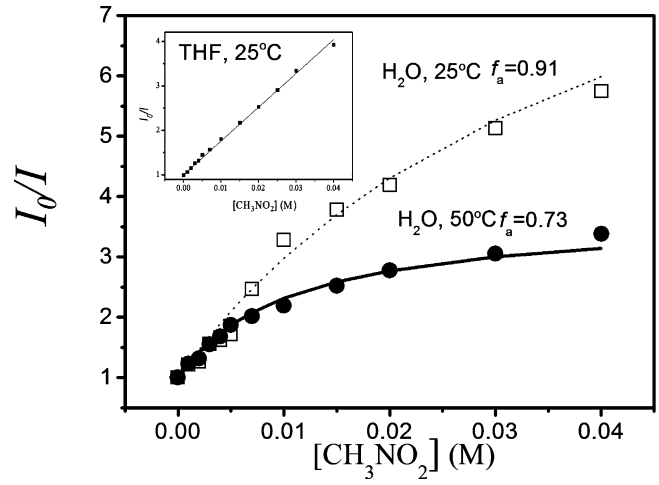

Figure 15. Ratio I_0/I of pyrene monomer emission intensity in the presence of the nitromethane compound in THF solution (shown in the inset), and in aqueous solutions of PGMA-*g*-Py/PNIPAM$_{53}$ at 25 and 50 °C. The polymer concentration was 0.068 g/L (pyrene moiety concentration is 10^{-5} M).

where I_0 and I are the pyrene monomer emission intensities in the absence and in the presence of the quencher; [Q] is the concentration of the quencher; K_{SV} is the Stern−Volmer quenching constant; and f_a is the percentage of the chromophores that are accessible to the quencher. We performed quenching experiments with nitromethane, a water-soluble compound, as the quencher to study the protecting effect of PNIPAM brushes on pyrene groups in the walls of vesicles. Figure 15 shows the changes of I_0/I with the concentration of the quencher at two temperatures. The nonlinearity of the two plots obtained at 25 and 50 °C indicates that the pyrene groups are not 100% accessible to the quencher in both cases, which is different from PGMA-*g*-Py/PNIPAM$_{53}$ in THF solution. In THF, I_0/I changes linearly with the concentration of the quencher (the inset in Figure 15), which means all the pyrene groups on PGMA-*g*-Py/PNIPAM$_{53}$ can be quenched in THF.[14] Comparing the values of I_0/I obtained at 50 °C, the higher intensity ratios measured at 25 °C indicate a higher quenching efficiency at a temperature below the LCST. The modified Stern−Volmer model was used to fit the two curves. The percentages of the chromophores which are accessible to the quencher were calculated. Our results show that 91% of pyrene groups in vesicular structures are

accessible to the quenchers at 25 °C, while only 73% of pyrene groups are accessible at 50 °C. When the temperature is above the LCST of PNIPAM, the collapsed PNIPAM side chains on the surface of the vesicles prevent the penetration of the nitromethane compound into the wall of vesicles, and a part of the pyrene groups were protected from being quenched.

4. Conclusions

A combination of click chemistry and RAFT polymerization is an efficient method in the synthesis of an amphiphilic asymmetric comb polymer with pendant pyrene groups and PNIPAM side chains. The comb polymer conformation is related to the polymer concentration in a good solvent. The pendant pyrene groups on the comb polymer form intramolecular excimer at low concentration and form intermolecular aggregation at high concentration. In a selective solvent, when the polymer concentration is above CAC, the comb polymer chains self-assemble into vesicles with pendant pyrene groups inside walls and PNIPAM side chains in the coronae. At a temperature above the LCST of PNIPAM, the PNIPAM side chains collapse forming nanosized domains on the surface of the vesicles. The collapsed PNIPAM chains protect a part of the pyrene groups from being quenched by nitromethane.

Acknowledgment. This project was supported by the National Natural Science Foundation of China (NSFC) under Contract No. 20774046.

Supporting Information Available: ^{1}H NMR spectra of the precursors of the comb polymer and more fluorescent spectra of the comb polymer in solution. This material is available free of charge via the Internet at http://pubs.acs.org.

References and Notes

(1) Heskins, M.; Guillet, J. E. *J. Macromol. Sci., Part A* **1968**, *2*, 1441–1455.
(2) Milewska, A.; Szydlowski, J.; Rebelo, L. P. N. *J. Polym. Sci., Part B* **2003**, *41*, 1219–1233.
(3) Rebelo, L. P. N.; Visak, Z. P.; de Sousa, H. C.; Szydlowski, J.; de Azevedo, R. G.; Ramos, A. M.; Najdanovic-Visak, V.; da Ponte, M. N.; Klein, J. *Macromolecules* **2002**, *35*, 1887–1895.
(4) Schild, H. G. *Prog. Polym. Sci.* **1992**, *17*, 163–249.
(5) Dong, L.; Agarwal, A. K.; Beebe, D. J.; Jiang, H. R. *Nature* **2006**, *442*, 551–554.
(6) Sidorenko, A.; Krupenkin, T.; Taylor, A.; Fratzl, P.; Aizenberg, J. *Science* **2007**, *315*, 487–490.
(7) Cheng, Z. Y.; Liu, S. H.; Beines, P. W.; Ding, N.; Jakubowicz, P.; Knoll, W. *Chem. Mater.* **2008**, *20*, 7215–7219.
(8) Das, M.; Mardyani, S.; Chan, W. C. W.; Kumacheva, E. *Adv. Mater.* **2006**, *18*, 80–83.
(9) Ionov, L.; Stamm, M.; Diez, S. *Nano Lett.* **2006**, *6*, 1982–1987.
(10) Yang, M.; Chu, L. Y.; Wang, H. D.; Xie, R.; Song, H.; Niu, C. H. *Adv. Funct. Mater.* **2008**, *18*, 652–663.
(11) Hong, S. W.; Kim, D. Y.; Lee, J. U.; Jo, W. H. *Macromolecules* **2009**, *42*, 2756–2761.
(12) Tang, L.; Jin, J. K.; Qin, A. J.; Yuan, W. Z.; Mao, Y.; Mei, J.; Sun, J. Z.; Tang, B. Z. *Chem. Commun.* **2009**, 4974–4976.
(13) Barros, T. C.; Adronov, A.; Winnik, F. M.; Bohne, C. *Langmuir* **1997**, *13*, 6089–6094.
(14) Winnik, F. M. *Macromolecules* **1990**, *23*, 1647–1649.
(15) Xu, J.; Zhu, Z. Y.; Luo, S. Z.; Wu, C.; Liu, S. Y. *Phys. Rev. Lett.* **2006**, *96*, 027802.
(16) (a) Sheiko, S.; Möller, M. *Chem. Rev.* **2001**, *101*, 4099–4123. (b) Sheiko, S.; Sumerlin, B. S.; Matyjaszewski, K. *Prog. Polym. Sci.* **2008**, *33*, 759–785. (c) Bhattacharya, A.; Misra, B. N. *Prog. Polym. Sci.* **2004**, *29*, 767–814.
(17) Subbotin, A.; Saariaho, M.; Ikkala, O.; ten Brinke, G. *Macromolecules* **2000**, *33*, 3447–3452.
(18) (a) Ma, Y. H.; Cao, T.; Webber, S. E. *Macromolecules* **1998**, *31*, 1773–1778. (b) Qi, H. F.; Zhong, C. L. *J. Phys. Chem. B* **2008**, *112*, 10841–10847.
(19) Thompson, C. J.; Ding, C. X.; Qu, X. Z.; Yang, Z. Z.; Uchegbu, I. F.; Tetley, L.; Cheng, W. P. *Colloid Polym. Sci.* **2008**, *286*, 1511–1526.
(20) Yang, B. S.; Lal, J.; Kohn, J.; Huang, J. S.; Russel, W. B.; Prud'homme, R. K. *Langmuir* **2001**, *17*, 6692–6698.
(21) Coessens, V.; Pintauer, T.; Matyjaszewski, K. *Prog. Polym. Sci.* **2001**, *26*, 337–377.
(22) Iha, R. K.; Wooley, K. L.; Nystrm, A. M.; Burke, D. J.; Kade, M. J.; Hawker, C. J. *Chem. Rev.* **2009**, *109*, 5620–5686.
(23) Matyjaszewski, K. *Controlled/LiVing Radical Polymerizations Progress in ATRP, NMP and RAFT*; American Chemical Society: Washington, DC, 2000.
(24) Kolb, H. C.; Finn, M. G.; Sharpless, K. B. *Angew. Chem., Int. Ed.* **2001**, *40*, 2004–2021.
(25) Rostovtsev, V. V.; Green, L. G.; Fokin, V. V.; Sharpless, K. B. *Angew. Chem., Int. Ed.* **2002**, *41*, 2596–2599.
(26) Tornoe, C. W.; Christensen, C.; Meldal, M. *J. Org. Chem.* **2002**, *67*, 3057–3064.
(27) (a) Zhang, X.; Lian, X.; Liu, L.; Zhang, J.; Zhao, H. *Macromolecules* **2008**, *41*, 7863–7869. (b) Wu, D.; Song, X.; Tang, T.; Zhao, H. *J. Polym. Sci., Part A: Polym. Chem.* **2010**, *48*, 443–453.
(28) Lai, J. T.; Filla, D.; Shea, R. *Macromolecules* **2002**, *35*, 6754–6756.
(29) Canamero, P. F.; de la Fuente, J. L.; Madruga, E. L.; Fernandez-Garcia, M. *Macromol. Chem. Phys.* **2004**, *205*, 2221–2228.
(30) Tsarevsky, N. V.; Bencherif, S. A.; Matyjaszewski, K. *Macromolecules* **2007**, *40*, 4439–4445.
(31) Winnik, F. M. *Chem. Rev.* **1993**, *93*, 587–614.
(32) Deepak, V. D.; Asha, S. K. *J. Phys. Chem. B* **2009**, *113*, 11887–11897.
(33) The "inner filter effect" is defined as "an apparent decrease in emission quantum yield and/or distortion of bandshape as a result of reabsorption of emitted radiation in an emission experiment" (http://www.iupac.org/goldbook/I03047.pdf).
(34) Char, K.; Frank, C. W.; Gast, A. P.; Tang, W. T. *Macromolecules* **1987**, *20*, 1833–1838.
(35) Siu, H.; Prazeres, T. J. V.; Duhamel, J.; Olesen, K.; Shay, G. *Macromolecules* **2005**, *38*, 2865–2875.
(36) Birks, J. B. *Photophysics of Aromatic Molecules*; Wiley: New York, 1970.
(37) Winnik, F. M.; Regismond, S. T. A. *Colloids Surf.* **1996**, *118*, 1–39.
(38) Yan, J.; Ji, W.; Chen, E.; Li, Z.; Liang, D. *Macromolecules* **2008**, *41*, 4908–4913.
(39) Wu, C.; Zhou, S. *Macromolecules* **1995**, *28*, 8381–8387.
(40) Liang, D.; Zhou, S.; Song, L.; Zaitsev, V. S.; Chu, B. *Macromolecules* **1999**, *32*, 6326–6332.
(41) Ding, Y.; Ye, X.; Zhang, G. *Macromolecules* **2005**, *38*, 4403–4408.
(42) Wu, C.; Wang, X. H. *Phys. Rev. Lett.* **1998**, *80*, 4092–4094.
(43) (a) Xia, Y.; Yin, X.; Burke, N, A. D.; Stöver, H. D. H. *Macromolecules* **2005**, *38*, 5937–5943. (b) Fujishige, S.; Kubota, K.; Ando, I. *J. Phys. Chem.* **1989**, *93*, 3311–3313.
(44) Zhang, W.; Zhou, X.; Li, H.; Fang, Y.; Zhang, G. *Macromolecules* **2005**, *38*, 909–914.

JP1007494